applied sciences

MDPI

Article

Spatial Assessment of Soil Erosion Risk Using RUSLE Embedded in GIS Environment: A Case Study of Jhelum River Watershed

Muhammad Waseem [1,*], Fahad Iqbal [1], Muhammad Humayun [1], Muhammad Umais Latif [1], Tayyaba Javed [1] and Megersa Kebede Leta [2,*]

[1] Department of Civil Engineering, Ghulam Ishaq Khan Institute of Engineering Science and Technology, Topi 23640, Pakistan
[2] Faculty of Agriculture and Environmental Sciences, University of Rostock, 18059 Rostock, Germany
* Correspondence: muhammad.waseem@giki.edu.pk (M.W.); megersa.kebede@uni-rostock.de (M.K.L.)

Abstract: The watershed area of the Mangla Reservoir spans across the Himalayan region of India and Pakistan, primarily consisting of the Jhelum River basin. The area is rugged with highly elevated, hilly terrain and relatively thin vegetation cover, which significantly increases the river's sediment output, especially during the monsoon season, leading to a decline in the reservoir's storage capacity. This work assesses the soil erosion risk in the Jhelum River watershed (Azad Jammu and Kashmir (AJ&K), Pakistan) using the Revised Universal Soil Loss Equation of (RUSLE). The RUSLE components, including the conservation support or erosion control practice factor (P), soil erodibility factor (K), slope length and slope steepness factor (LS), rainfall erosivity factor (R), and crop cover factor (C), were integrated to compute soil erosion. Soil erosion risk and intensity maps were generated by computing the RUSLE parameters, which were then integrated with physical factors such as terrain units, elevation, slope, and land uses/cover to examine how these factors affect the spatial patterns of soil erosion loss. The 2021 rainfall data were utilized to compute the rainfall erosivity factor (R), and the soil erodibility (K) map was created using the world surface soil map prepared by the Food and Agriculture Organization (FAO). The slope length and slope steepness factor (LS) were generated in the highly rough terrain using Shuttle Radar Topography Mission Digital Elevation Model (SRTM DEM). The analysis revealed that the primary land use in the watershed was cultivated land, accounting for 27% of the area, and slopes of 30% or higher were present across two-thirds of the watershed. By multiplying the five variables, the study determined that the annual average soil loss was 23.47 t ha^{-1} yr^{-1}. In areas with dense mixed forest cover, soil erosion rates ranged from 0.23 t ha^{-1} yr^{-1} to 25 t ha^{-1} yr^{-1}. The findings indicated that 55.18% of the research area has a low erosion risk, 18.62% has a medium erosion risk, 13.66% has a high risk, and 11.6% has a very high erosion risk. The study's findings will provide guidelines to policy/decision makers for better management of the Mangla watershed.

Keywords: Mangla catchment; RUSLE; GIS; IRS LISS III; LANDSAT 8

Citation: Waseem, M.; Iqbal, F.; Humayun, M.; Umais Latif, M.; Javed, T.; Kebede Leta, M. Spatial Assessment of Soil Erosion Risk Using RUSLE Embedded in GIS Environment: A Case Study of Jhelum River Watershed. *Appl. Sci.* **2023**, *13*, 3775. https://doi.org/10.3390/app13063775

Academic Editors: Wojciech Zgłobicki and Leszek Gawrysiak

Received: 31 January 2023
Revised: 9 March 2023
Accepted: 10 March 2023
Published: 15 March 2023

1. Introduction

Soil erosion is a significant global environmental issue that has far-reaching impacts. It reduces soil productivity, causes the loss of essential nutrients, and leads to siltation in water bodies, further exacerbating the problem [1]. Additionally, soil erosion has severe effects on public health and the livelihoods of marginalized communities, especially those reliant on agriculture. Therefore, addressing soil erosion is crucial to mitigate its damaging effects on the environment and society [2]. Soil erosion by water is one of the most common problems, second only to climate change, that requires attention [3–5]. Soil erosion poses a significant risk to the northern regions of Pakistan, including AJ&K, due to various factors such as heavy rainfall, land susceptibility, overgrazing, and human activities that contribute

to the problem. These activities include overpopulation, deforestation for agriculture, high urban demands, as well as the extraction of wood and raw materials [6–9].

Mangla and Tarbela watersheds are among the most vital water resources in Pakistan [10]. The Upper Jhelum Basin is the catchment area of the Mangla Reservoir, which is made up of high hills and relatively sparse vegetation. Particularly during the monsoon season (July to September), a large amount of silt is generated in the basin. This is due to heavy rainfall during monsoons, which leads to a high silt yield in the river [11]. Because of its morphology, the basin is exposed to landslides, floods, and earthquakes and is extremely prone to soil degradation [12]. The effects of land erosion on Mangla Dam are significant and far-reaching, impacting crucial areas such as agriculture, waterways, and infrastructure in the country [13,14]. In particular, the physical stress caused by land erosion hinders the development of agriculture in the country, as it undermines the ability of farmers to grow crops and support their livelihoods. This underscores the urgent need to address land erosion to ensure the sustainability of agriculture and other vital sectors [15]. Additionally, the erosion leads to a reduction in water-holding capacity and soil nutrient accumulation, which inhibits the regrowth of vegetation [16,17].

Globally, land erosion leads to an estimated $7 billion in damages to farms annually due to increased flooding [18,19]. This damage extends to public and industrial water storage facilities, water-based recreation areas, and more. Sediments also contribute to increased flood risks and infrastructural damage, affecting roads, dams, buildings, and utility networks [20–23]. Over the past century, land degradation has intensified, resulting in the loss of approximately twenty-four million tons of productive topsoil from agricultural lands worldwide [24]. According to the United Nations Food and Agriculture Organization, 90% of the Earth's precious topsoil will likely be at risk by 2050 [25].

Traditional soil erosion evaluation methods based on field surveys are labor-intensive, expensive, and time-consuming [26]. Therefore, a numerical evaluation technique is often desirable for developing regional management strategies to estimate the severity of soil erosion and quantify the amount of soil loss, enabling better management strategies to be developed. This provides an alternative way to study and simulate the long-term and short-term consequences of land use activities on the natural system [27] and to assess other land management strategies in gauged and ungauged basins. Effective use of land resources can also be achieved by developing several land use cases and evaluating their results using soil erosion models [28–30]. These models have been developed and used for more than seven decades, with examples including the Water Erosion Prediction Project (WEPP) [31–33], the Soil and Water Assessment Tool (SWAT) [31,34], the revised model of Morgan and Finney (RMMF) [35], the Soil Erosion Model for Mediterranean Regions (SEMMED) [31], and the European Soil Erosion Model EUROSEM. There are several levels of complexity in these models, with the most popular empirical model used to estimate soil erosion being the Universal Soil Loss Equation (USLE) [26]. The USLE model was revised and digitized in the early 1990s to produce the Revised Universal Soil Loss Equation (RUSLE), which is widely used to predict soil erosion [36–38]. The Universal Soil Loss Equation (USLE) and Revised Universal Soil Loss Equation (RUSLE) [39,40] are mostly used worldwide under a variety of circumstances. The three categories of soil erosion models are empirical, conceptual (partially empirical/mixed), and physical, with USLE and RUSLE being classified as empirical and conceptual (partly empirical) based models [41]. The RUSLE model has been used for more than 80 years due to its good reliability, ease of applicability, high degree of flexibility, correctness, and data accessibility [42–48]. The current study used RUSLE Model and Geo-Information tools to quantify soil erosion.

The aim of this study is to utilize the revised Universal Soil Loss Equation and geographic information techniques for the following purposes: (i) to calculate the potential soil loss in the Jhelum River watershed, (ii) to create maps of soil erosion risk and severity, and (iii) to identify areas with critical soil erosion conditions that necessitate immediate conservation and land management measures. The study shall help the authorities in the adaptation of adequate measures and best management practices for soil and water

conservation in the zones with high erosion risk. The method of the applied RUSLE model in combination with GIS can be transferred at the desired rate of complexity to similar catchments in the south Asian region.

2. Study Area

The Jhelum River basin, as shown in Figure 1, extends from 33°3′ N–35°9′ N and 73°8′ E–75°35′ E and originates in the rugged mountain ridge of the upper part of the Kashmir valley [11]. After the River Indus, the upper Jhelum river is the second-largest tributary of the Indus basin [49]. The watershed's drainage area is 33,563 km^2, and the altitude varies from 264 to 6304 m. The entire basin ultimately flows into the Mangla Reservoir, which is Pakistan's second-largest reservoir, constructed in 1967. The primary function of this dam is irrigation, which serves about 6 million hectares of land. Additionally, the dam serves as a hydropower generator, with a current capacity of 1000 MW, contributing to 6% of the country's overall installed hydropower generation capacity [50].

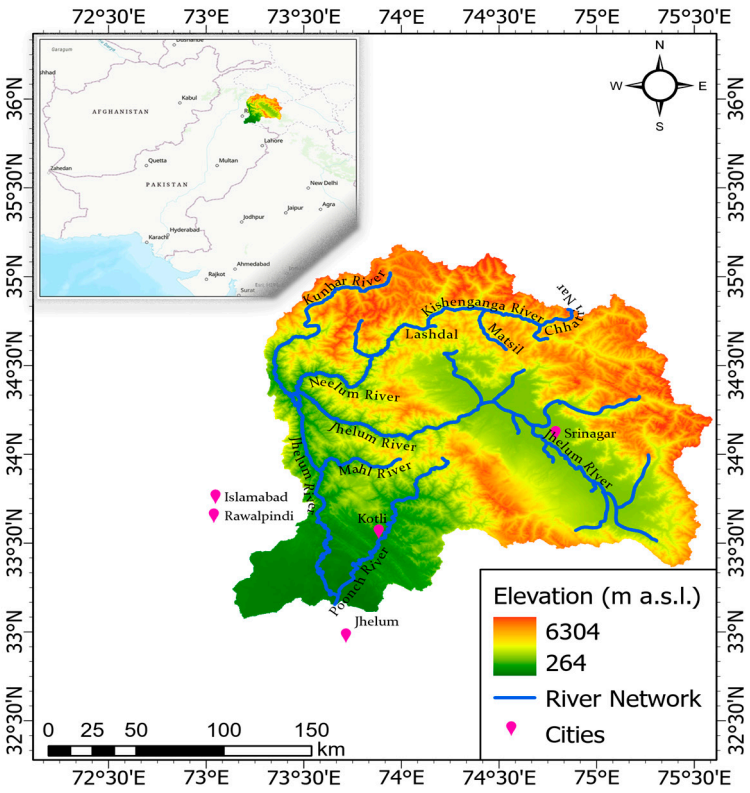

Figure 1. Location of the study area.

Due to its morphology, the Jhelum River basin is highly susceptible to soil erosion, in addition to being extremely sensitive to landslides, floods, and earthquakes. Human-caused threats, such as overgrazing, deforestation for agricultural purposes, increasing urbanization, and mining activities, also contribute to the vulnerability of the Jhelum watershed [51]. This study focused on analyzing the Jhelum River basin, which is not only important for the country but is also facing extreme soil erosion due to anthropogenic and climate change activities.

3. Methodology

3.1. RUSLE Equation

Soil erosion is a complex phenomenon that can be studied through various models, including the widely used universal soil loss equation (USLE). The empirical nature of the revised universal soil loss equation (RUSLE) makes it a suitable approach for analyzing

soil erosion. Using this approach, cartographic maps can be created to understand soil erosion in specific regions, with several parameters directly or indirectly linked to soil erosion [52,53]. Directly linked parameters such as slope length and steepness, rainfall intensity, and soil erodibility factor impact soil loss, while indirectly linked parameters such as crop management practices and soil conservation practices impact soil loss by influencing the direct parameters [54]. By predicting USLE parameters and creating cartographic maps, the model gains insights into erosion in vulnerable areas [55]. In this study, the RUSLE model was applied using a land cover map created from remotely sensed satellite data, soil types, and agricultural practices. One of the model's main characteristics is that it can be easily incorporated into GIS for improved analysis, making it a valuable option for this study. The methodology followed during this study is depicted in Figure 2, with the RUSLE equation (Equation (1)) developed by combining five input parameters that are interrelated and subject to variations in both space and time. The input data for each element depends on one another and can change over time and space, leading to the calculation of erosion at a pixel level.

$$A = R \times K \times LS \times C \times P \quad (1)$$

where A, average annual soil erosion ($t \cdot ha^{-1} \cdot y^{-1}$); R, rainfall erosivity factor ($MJ \cdot mm \cdot ha^{-1} \cdot h^{-1} \cdot y^{-1}$); K, erodibility of soil ($t \cdot ha^{-1} \cdot h \cdot MJ^{-1} \cdot ha^{-1} \cdot mm^{-1}$); the rest of parameters are dimensionless as shown in Figure 2.

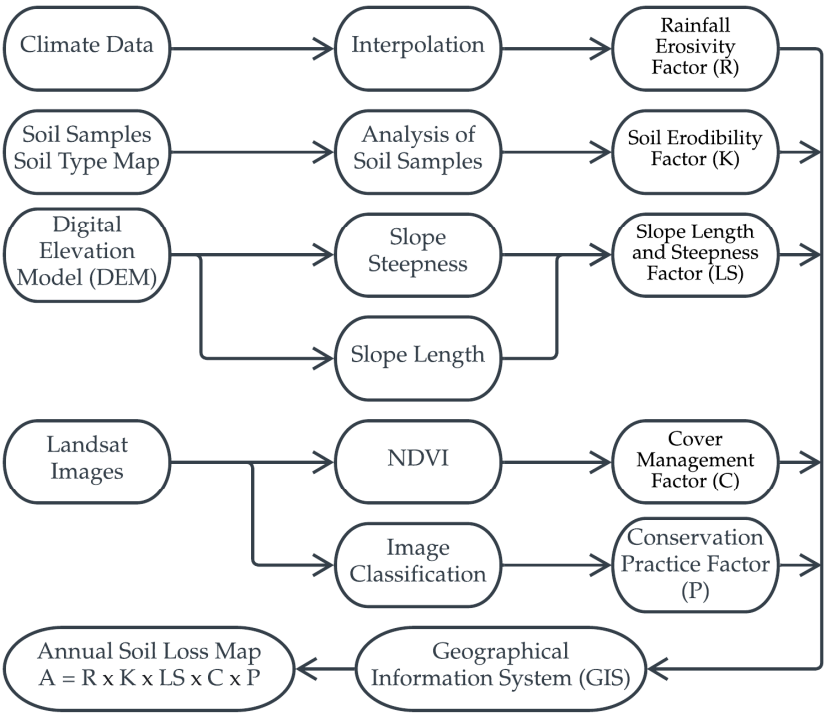

Figure 2. The methodological framework of the current research study.

All these five contributing factors were incorporated individually in ArcGIS, and then the soil erosion was estimated empirically using the raster map function. The boundaries of the study area were set by using the spatial function of ArcGIS. The entire spatial and remotely sensed data were processed using ArcGIS Pro 2.8.0 software. The RUSLE parameters were calculated using satellite imagery, and digital elevation model data are shown in Table 1.

Table 1. Sources of remotely sensed data.

Sr. No.	Type of Data	Description	Source
1	DEM	SRTM DEM 1 Arc-Second Global with spatial resolution of 30 m	USGS Earth Resources Observation and Science [56]
2	Soil Data	Digital soil Map of the World by FAO spatial resolution of 5 × 5′	Food and Agriculture Organization of the United Nations [57]
3	Rainfall Data	CRU TS Monthly High-Resolution Gridded Multivariate Climate Dataset Spatial resolution 0.5°	Climatic Research Unit (University of East Anglia) and Met Office [58]
4	Satellite Data	Landsat 8-9 OLI/TIRS Collection 2 with spatial resolution of 30 m	USGS Earth Resources Observation and Science [56]

3.2. Rainfall Erosivity Factor-R

R-factor plays a main role in RUSLE. This factor is a major cause of soil erosion and represents the erosivity of rainfall over time. It measures the amount of soil erosion in response to precipitation at a specific place. For soil erosion evaluation, the R-factor is crucial when land use and climate scenarios are changing [59–61]. It determines the effect of rainfall and runoff rate [62,63].

In order, to compute the R-factor, the Annual and monthly rainfall data for the Jhelum Basin watershed were used. After the data were imported into a GIS system, the yearly rainfall data from the netCDF raster were converted to point data, and then the Kriging interpolation method was applied to generate the Precipitation map. The monthly R-factor was computed by Equation (2), developed by Smith and Wischmeier [39] and revised by Arnoldus [64].

$$R = \sum_{i=1}^{12} 1.735 \times 10 \times \{1.5 \times \log_{10}\left\{\frac{P_i^2}{P}\right\} - 0.08188\} \quad (2)$$

where, R (MJ·mm·ha $^{-1}$·h^{-1}·y $^{-1}$) shows the rainfall erosivity, P_i for the rainfall (mm) occurring each month, and P stands for the rainfall (mm) occurring annually. Mean annual rainfall and distribution of rainfall erosivity (R-factor) are shown in Figure 3a,b, respectively. For the study area, the value of R ranges between 544.8 and 766.8, with a minimum value of 267.26 and a maximum of 2043.

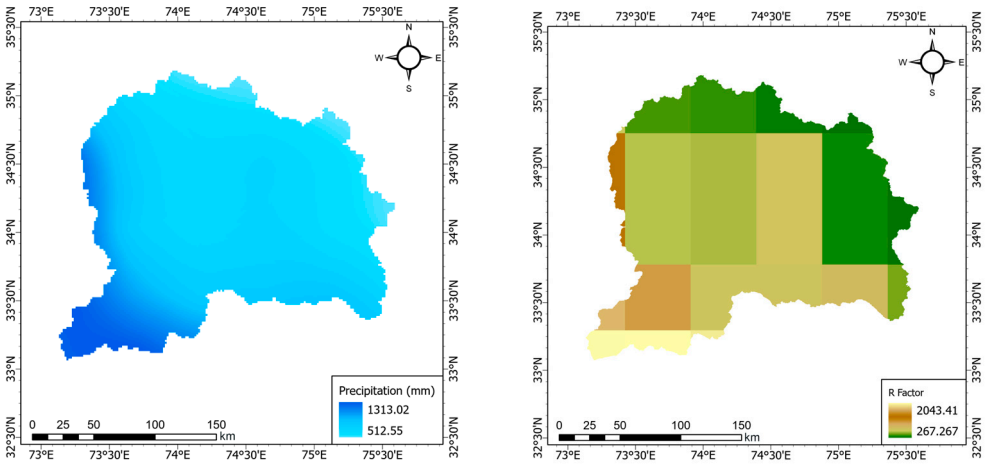

(**a**) (**b**)

Figure 3. (**a**) Map of mean annual rainfall; (**b**) distribution of rainfall erosivity (R-factor).

3.3. Soil Erodibility Factor-K

The K-factor represents the typical long-term response of soil to rainfall and runoff. This concept can be further supported by the fact that rainfall detaches soil particles, which are then carried away by runoff. The repeated occurrence of this process over time results in soil erosion, which is numerically estimated using the K-factor. This factor specifies the soil loss for a specific soil type with a unit rainfall erosion index. The USLE model employs Wischmeier's method to calculate the K-factor, which takes into account various soil characteristics such as soil size, level of organic matter, structure, and porosity of particles [27,28]. In order to prepare a soil profile for the study area, the FAO digital soil map for the world was utilized. The soil map for the study area was obtained using the "clip features" function in ArcGIS Pro 2.8.0. The corresponding K-factors were calculated for each soil type using Equations (3)–(7) proposed by Williams [65]:

$$K_{usle} = f_{csand} \times f_{cl-si} \times f_{orgc} \times f_{hisand} \quad (3)$$

$$f_{csand} = (0.2 + 0.3 \times \exp(-0.256 \times m_s(1 - \frac{m_{silt}}{100}))) \quad (4)$$

$$f_{cl-si} = \left(m_{silt}/(m_c + m_{silt})\right)^{0.3} \quad (5)$$

$$f_{orgc} = (1 - \frac{0.25 \times orgc}{orgc + \exp(3.72 - 2.95 \times orgc)}) \quad (6)$$

$$f_{hisand} = (1 - \frac{0.7 \times (1 - \frac{m_s}{100})}{(1 - \frac{m_s}{100}) + \exp(-5.51 + 22.9 \times (1 - m_s/100))}) \quad (7)$$

where, K_{usle} represents the factor of erodibility, m_s represents the percent sand, m_{silt} represents the percent silt, m_c represents the percent clay, and f_{orgc} reduces K values in soil with high organic carbon content, $orgc$ shows organic carbon content, f_{csand} is a factor that lowers the K indicator in soils with high coarse-sand content and higher for soil with little sand, f_{cl-si} gives low soil erodibility factors for soils with high clay-to-silt ratios, f_{hisand} lowers the K value for soils with extremely high sand content. The corresponding K-factor was computed for each soil type, and the values were entered in the raster table of ArcGIS. By using these values, a K-factor map was generated. The values calculated for each soil type are provided in Table 2.

Table 2. K-factor values for different soil types of the study area.

Sr. No.	Soil Sample	FAO Soil Class	K-Factor
1	BE	Eutric Cambisols	0.15
2	I	Lithosols	0.14
3	LO	Orthic Luvisols	0.13
4	RC	Calcaric Regosols	0.16
5	GL	Glacier	1
6	WR	Inland water or ocean	0

The map in Figure 4a,b illustrates the Jhelum watershed's soil type and K factor, respectively; typical K values range from 0.131 to 0.156.

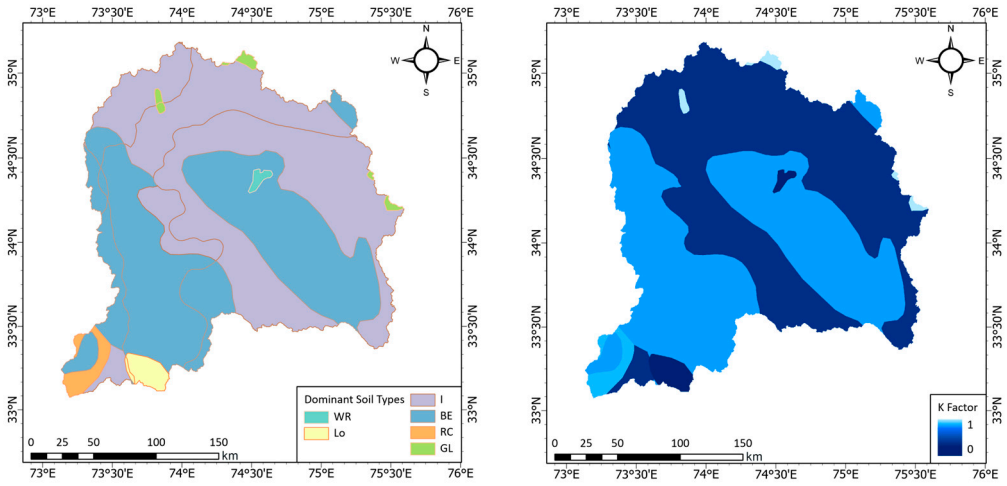

(**a**) (**b**)

Figure 4. (**a**) Maps of Soil type; (**b**) Soil erodibility (K-factor).

3.4. LS-Factor

In USLE, the L and S factors represent the effects of topography on the erosion rate. Higher slope length and slope steepness factors represent more overland flow and more soil erosion [66]. Moreover, slope variations have a much more significant impact on gross soil loss than slope length variations [67]. Topography is an important factor, especially when the ground slope increases beyond the critical angle. In order to obtain the LS factor for the Mangla watershed, the digital elevation model (DEM) was used in the ArcGIS environment. This is because the DEM provides the slope length and slope steepness of the terrain, which are necessary inputs for calculating the LS factor. It is necessary to account for variables such as flow accumulation and slope steepness while computing LS. The slope steepness and flow accumulation parameters were incorporated through the digital elevation model through the ArcGIS Spatial analyzer extension. From this digital elevation model, runoff accumulation and slope were computed. The LS-factor was computed using Equation (8) as suggested by Moore and Burch [68,69].

$$\mathrm{LS} = \frac{(\mathrm{Flowaccumulation} \times \mathrm{CellSize})^{0.4}}{22.13} \times \frac{(\mathrm{SinSlope})^{1.3}}{0.0896} \tag{8}$$

where, flow accumulation represents the cumulative upslope supporting area for a cell, the LS factor represents the factor of slope length along with slope steepness, Cell Size represents the size of the grid cell, and the slope degree is represented by 'Sin slope' whose value is in sin. The slope classification map and value of the LS factor is illustrated in Figure 5a,b, respectively.

3.5. C-Factor (Crop Cover Factor)

The C-factor ranges from 0 to 1 [11], and it characterizes the vegetation cover percentage and crop's influence on soil erosion. Vegetation coverage is considered a key factor in preventing water erosion. In order to quantify vegetation cover indices, the Normalized Difference Vegetation Index (NDVI) is used [11,49]. NDVI establishes a relation between soil erosion on land with no vegetation and soil erosion under certain vegetation. It also highlights cover type and density's impacts on preserving soil. A C-factor map was generated by using Equation (9).

$$\mathrm{NVDI} = \frac{\mathrm{NIR} - \mathrm{Red}}{\mathrm{NIR} + \mathrm{Red}} \tag{9}$$

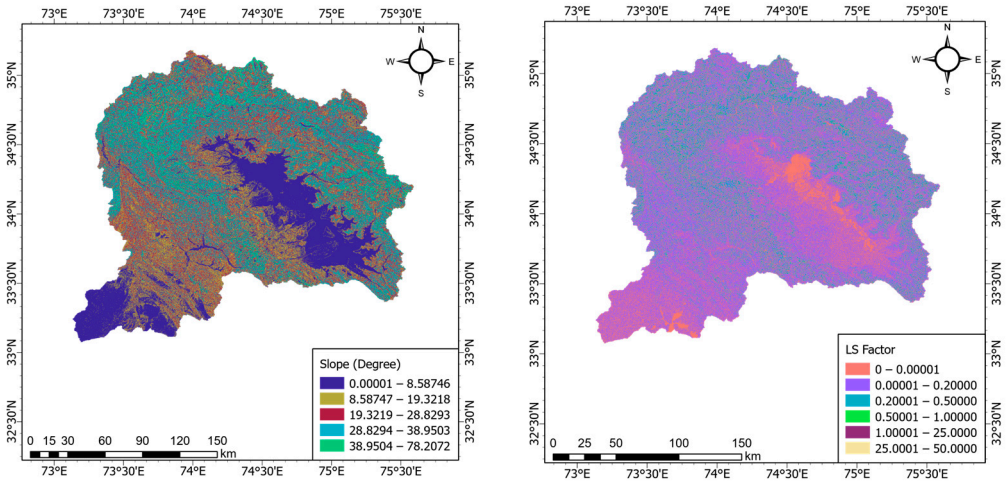

(**a**) (**b**)

Figure 5. (**a**) Slope Classification Map; (**b**) LS-factor Map.

NDVI stands for normalized difference vegetation index, NIR represents the near-infrared band, and Red represents the red band of the satellite image. Landsat 8-9 OLI/TIRS images with a spatial resolution of 30 m were utilized to estimate vegetative density. A Normalized Difference Vegetation Index (NDVI) was computed from Landsat images to approximate greenery. C factor was estimated by using Equations (10) and (11) [70,71], shown below.

$$\text{C factor} = 0.450 - 0.805 \times \text{NDVI} \tag{10}$$

$$\text{C factor} = \frac{(-\text{NDVI} + 1)}{2} \tag{11}$$

More than 60% of the watershed is covered by vegetation and trees, resulting in a lower C-factor. Conversely, the C-factor is higher in the northeastern parts of the area, which consists of clean land and glaciers. The land use and corresponding C-factor values, as shown in Figure 6a,b, illustrate the variation in vegetation cover and its influence on erosion across the study area.

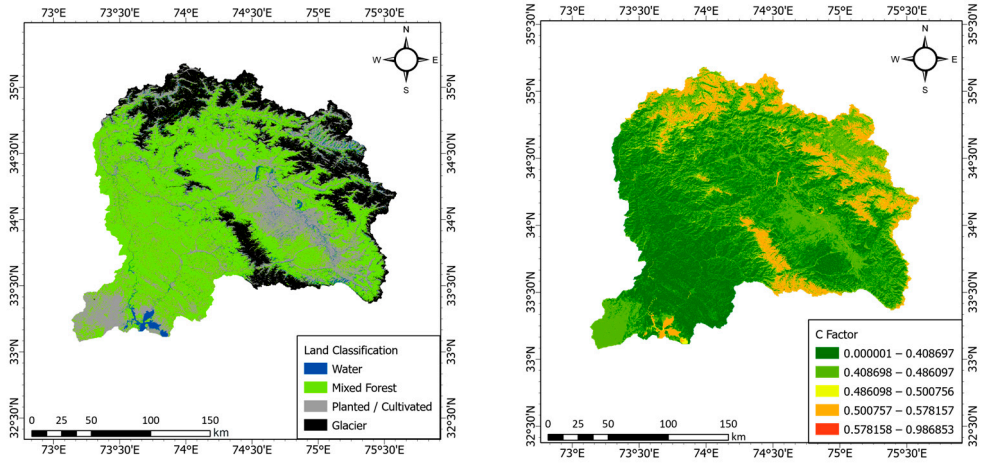

(**a**) (**b**)

Figure 6. (**a**) Land use; (**b**) land cover management (C-factor) map.

3.6. P-Factor (Conservation Practice Factor)

The P factor governs the soil loss ratio caused by uphill and downhill tillage, and it is used to adjust the USLE estimate for management and tillage operations to prevent

soil erosion [40]. The map of this factor was obtained from the percent slope and land use, and land classification was performed using supervised classification in the ArcGIS environment. Once the land was classified, the slope classes were combined, and the P-conservation factor was assigned to the defined slope classes [39,72].

The typical values of the P factor range between 0.1 and 1, as shown in Figure 7. Non-conservation practices result in higher values, while areas with plantations result in lower values. Based on the results, the core zone of the study area has lower *p* values, while larger values were found in the top part of the catchment. A conservation value of 0.1 characterizes durable safety capability against erosion resulting from human intervention, and 1 represents no capability for protection [73].

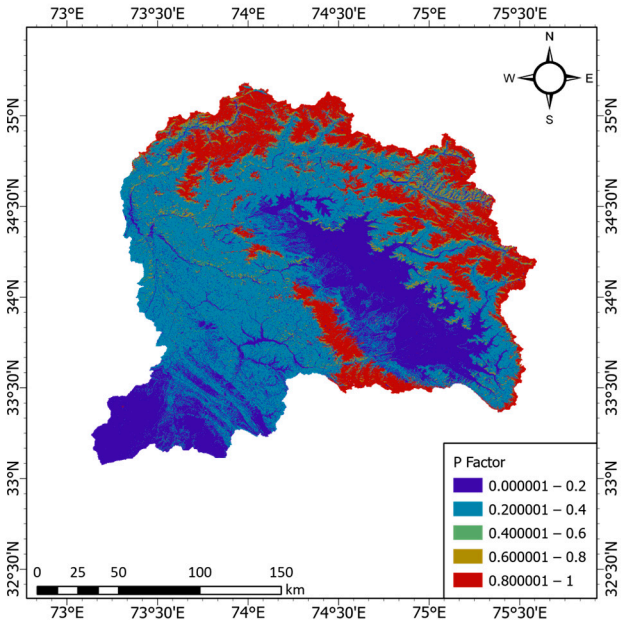

Figure 7. The conservation practice (P-factor).

4. Results and Discussion

4.1. Annual Average Soil Loss

This study finds the annual soil erosion for the Jhelum River catchment based on rainfall data for the year 2021 at 1 km^2 spatial resolution. We used all the geospatial data available for our study area and selected the RUSLE model as a cost-effective and easily applicable method for soil erosion estimation. Soil erosion risk maps were produced by consolidating all five parameters (LS, K, P, R, C) using Equation (1) in the spatial analyst tools, i.e., raster calculator ArcGIS. The map was calibrated and analyzed for the severity of soil risk in the watershed. A higher A value indicates a higher erosion rate, while a lower value indicates a softer sediment yield.

Figure 8 demonstrates all six categories created using the soil erosion and severity map based on previous studies in the same area [74]. 55% of the watershed has very low soil erosion, followed by 19% for low, 14% for moderate, 8% for moderate-high, and 4% for high erosion risk, according to the study's categories for soil erosion risk, as shown in Table 3.

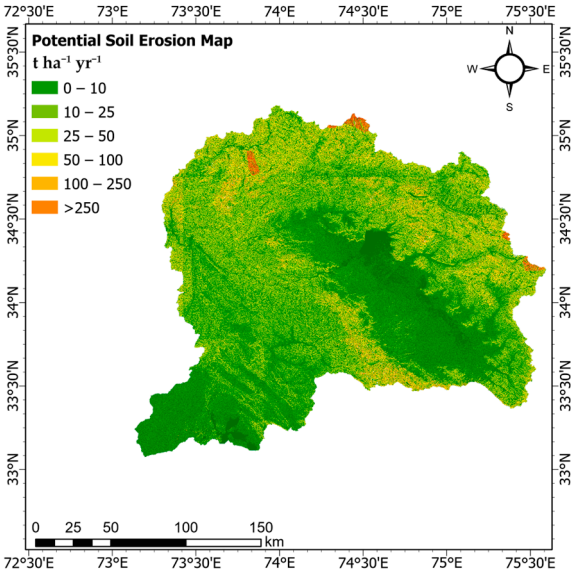

Figure 8. Erosion risk map of the entire watershed.

Table 3. Classification of soil erosion of Jhelum watershed concerning the area.

Range	Cell Count	Area km^2	Area %	Classes
0–10	1,852,243	18,522.43	55%	0–10 tons per hectare
10–25	625,111	6251.11	19%	10–25 tons per hectare
25–50	458,754	4587.55	14%	25–50 tons per hectare
50–100	281,068	2810.68	8%	50–100 tons per hectare
100–250	111,059	1110.59	3%	100–250 tons per hectare
250.00	28,149	281.49	1%	above 250 tons per hectare

4.2. Comparison with Global and Local Studies

The present study's findings were compared to those of similar studies conducted in nearby areas. Specifically, the first point of comparison was Borrelli et al.'s global soil ero-sion map, which utilized RUSLE 2017. This map was resampled to a scale of 25 km^2 by Gilani et al. to create soil erosion maps for various regions of Pakistan [75,76]. The re-ported soil erosion rate for AJ&K was taken into consideration and compared to the results of this study. To facilitate this comparison, the soil erosion map generated in the present study was resampled to a scale of 25 km^2 and then compared to past studies. Global soil erosion map showed significantly higher values than those estimated in this study (23.47 t ha^{-1} yr^{-1}). This fact stands true, especially with lower erosion values where our study re-ports 0–1 t ha^{-1} yr^{-1} erosion rates, the global map reports 4–5 t ha^{-1}yr^{-1}.

Due to similar topography and rainfall patterns, the soil erosion values reported in this study are within the range of soil erosion rates reported by other researchers in the adjoining areas and other countries. Table 4 highlights a comparison of the average soil erosion rates across various studies conducted at the watershed level. The analysis reveals that the soil erosion rates reported in Sediments rating curve SRC by Surface Water Hydrology Department (2005) [77], and Rawal watershed were lower than those observed in the present study [78]. In contrast, the Ghabbir watershed and national erosion map for Azad Jammu and Kashmir reported almost equal soil erosion in this watershed.

Table 4. Comparing soil erosion estimates in neighboring areas with similar topography using both global and local studies.

Reference	Study Area	Soil Erosion Rate (t ha^{-1} yr^{-1})
		Calculated by the Respective Local Study
Ashraf et al. [78]	Rawal watershed	10.3
	Ghabbir watershed	22
Aslam et al. [77]	Jhelum watershed	14
SRC's. [77]	Jhelum watershed	17.51
Borrelli et al. [75,76]	Azad Jammu and Kashmir	40.88
Gilani et al. [76]	Azad Jammu and Kashmir	22.25
Current Study	Jhelum watershed	23.47

The drainage area of the Rawal watershed is 268.69 km^2, while that of the Mangla watershed is 33,563 km^2. In the Rawal watershed, only 23% [NO_PRINTED_FORM] of the area has a slope of more than 30%, while in the Mangla watershed, the slope of most of the area ranges from 17% to 57% and reaches even 510% in some areas [79]. Because of these facts, the Rawal watershed has an annual average soil loss of 10.3 t ha^{-1} yr^{-1}, while the Mangla watershed has 23.47 t ha^{-1} yr^{-1} of annual average soil loss [78]. The Ghabir watershed drainage area is 417 km^2, with 85% of the area having gills and nullah [78]. Steep slopes, excessive hilly areas, and less vegetation are the causes of soil loss which is comparable with that of the Mangla watershed.

Furthermore, in previous studies, the soil loss for the Mangla watershed, as shown in Table 4, was calculated using USLE [26,77], whereas we used the RUSLE model. The discrepancy in soil loss values may be due to the fact that USLE does not consider land use and management practices, while RUSLE does. Additionally, differences in data accuracy and completeness and the time elapsed between both studies could also be driving factors for this difference.

Moreover, the soil loss in Azad Jammu and Kashmir is higher than in our study area due to the more rugged mountains and steep slopes, as well as the wetter climate with frequent rainfalls.

4.3. Primary Causes for Soil Loss, Land Use, and Land Cover Changes

From the research conclusions, the estimated soil erosion reported in earlier studies based on the data from 2005 and 2017 was 15 t ha^{-1} yr^{-1} which has increased to 23.47 t ha^{-1} yr^{-1} in 2021 [80].

The earthquake that occurred in the northern regions of Pakistan on 8 October 2005 resulted in a manifold increase in soil erosion in the area. This earthquake of magnitude 7.6 Mw (Moment Magnitude Scale) and its aftershocks were the sources of many landslides and soil erosion in the area [81]. Analysis shows that soil erosion has increased significantly near the epicenter of the earthquake. Moreover, soil erosion has also escalated due to the high average annual population growth rate of AJ&K (1.61%) [82] and the poor development of infrastructure [83]. The instability in the mountainous regions is further compounded by the fact that Pakistan has a forest cover of only 2.5%, and the annual deforestation rate is 2.1% [84]. Soil conservation methods face various challenges, including socioeconomic differences, violations of the law and court rulings, as well as a lack of awareness and education.

Due to poor rock weathering, increased surface runoff, and natural disasters, soil erosion increased manifold. Additionally, landslides and forest degradation significantly contributed to soil erosion at higher altitudes throughout the sixteen-year study period (2005–2015) [76].

The results indicate that soil erosion values are higher in areas with steep slopes near drainage lines such as streams and rivers. This could be due to runoff carrying large amounts of damaged materials. The steeper sections and higher slopes are also impacted by rills, gullies, and significant amounts of silt, which were easily observable during field surveys. These features are common in the research area due to their delicate geomorphology.

Moreover, the study found that areas with farming and dense mixed forests had the lowest erosion rates, whereas areas covered in snow and glacier patches had the highest rates of erosion [79].

4.4. Strengths and Limitations

The most applicable soil loss estimation model is RUSLE. Because it can predict soil loss using little information, this model is ideal for developing countries with scarce data. The results of other models are elaborate but difficult to interpret and validate due to their complex nature. Most other models are based on empirical rules, leaving much room for error [85]. This model identifies high-risk areas, and management actions are required immediately. It provides an easy-to-use, adaptable, and physical foundation for determining the relative soil loss pattern.

Despite its numerous advantages, the RUSLE model has certain limitations. This equation was established via regression analysis with little field data of similar nature regarding rain patterns, soil types, land cover, and topography [86]. In addition, since it was developed on datasets of the US, its application on a catchment in Pakistan can be questioned. Additionally, to use it for location outside the datasets on which the model was calibrated requires long-term data to calibrate and calculate its coefficients. Moreover, it is also known that gully or stream-channel erosion is not considered while calculating soil loss which is the governing factor in soil erosion. Finally, calculating soil erosion by merely multiplying various factors cannot achieve full accuracy because factors such as sediment deposition, routing, and sediment yield at the catchment outlet are not considered, resulting in inaccurate estimations [87].

5. Conclusions

This study attempted to produce the yearly soil erosion map for the Jhelum watershed using the RUSLE model in a GIS-embedded environment. Various data sources in ArcGIS were used to create RUSLE input parameters. By merging the model RUSLE with GIS techniques, the results of each factor contributing to the erosion process are displayed. Regarding the many elements contributing to land degradation, GIS allows the management of huge amounts of data relatively simply. It's obvious from this study that the GIS approach is straightforward, has a low cost for modeling and mapping soil erosion, and is very valuable for assessing soil erosion.

The combination of heavy rainfall and steep slopes in the study area results in significant erosion runoff. The primary cause of the huge soil erosion in our study area is the outcome of high runoff and soil particle dislodging. This study shows that 55.18% of this watershed has a low erosion risk, 18.62% of the area has a moderate erosion risk, 13.66% has a high risk, and 16% has a very high erosion risk. Moreover, this study finds that the annual average erosion for the Mangla watershed is 23.47 t ha^{-1} yr^{-1}.

Although soil loss in this area is comparatively low, effective management policies and strategies must be adopted to further reduce it, with a special focus on C and P. This is because the LS factor is influenced by topography, which cannot be easily changed on a larger scale, while the other two factors, R and K, cannot be changed [88]. This shall increase the life of the Mangla DAM to a greater extent, positively impacting Pakistan's agricultural and power sectors.

- Proper supervision of terraces will condense the length of the slope and, subsequently, the soil loss [89].

- By adopting innovative and sound cultivation methods, the C factor can be reduced, and erosion can be reduced.
- Conservation practices (P), such as curvature against the slope and trees on the field's boundary, will ensure that sediments do not leave their source [90].

Author Contributions: Conceptualization, F.I. and M.W.; methodology, F.I., M.H. and M.U.L.; software, F.I.; validation, F.I., M.H. and M.U.L.; formal analysis, T.J. and M.K.L.; investigation, M.W.; data curation, T.J.; writing—original draft preparation, F.I., M.H. and M.U.L.; writing—review and editing, M.W. and M.K.L.; visualization, T.J.; supervision, M.W. and M.K.L. All authors have read and agreed to the published version of the manuscript.

Funding: This study is not supported by any external funding. We are thankful to the University of Rostock, Open access program for their support in the payment of the article processing charges.

Institutional Review Board Statement: Not applicable.

Informed Consent Statement: Not applicable.

Data Availability Statement: To respect the privacy of the datasets generated and/or analyzed here, they are not publicly available. The author can provide the datasets upon reasonable request.

Acknowledgments: The authors of the study extend gratitude to ESRI and USGS for providing the land use, land cover data, and DEM for this research.

Conflicts of Interest: The authors declare no competing interests.

References

1. Pal, S.C.; Chakrabortty, R.; Roy, P.; Chowdhuri, I.; Das, B.; Saha, A.; Shit, M. Changing Climate and Land Use of 21st Century Influences Soil Erosion in India. *Gondwana Res.* **2021**, *94*, 164–185. [CrossRef]
2. UNCCD. *Elaboration of an International Convention to Combat Desertification in Countries Experiencing Serious Drought and/or Desertification, Particularly in Africa. United Nations, General Assembly*; UNCCD: Nairobi, Kenya, 1994.
3. Lal, R. Soil Degradation by Erosion. *Land Degrad. Dev.* **2001**, *12*, 519–539. [CrossRef]
4. Terranova, O.; Antronico, L.; Coscarelli, R.; Iaquinta, P. Soil Erosion Risk Scenarios in the Mediterranean Environment Using RUSLE and GIS: An Application Model for Calabria (Southern Italy). *Geomorphology* **2009**, *112*, 228–245. [CrossRef]
5. Eswaran, H.; Lal, R.; Reich, P.F. Land Degradation: An Overview. Responses to Land Degradation. In *Proceedings of the 2nd International Conference on Land Degradation and Desertification*; Oxford Press: New Delhi, India, 2019.
6. Soil and Water Conservation. Available online: https://www.fao.org/3/T0321E/T0321E00.htm (accessed on 19 November 2022).
7. Bou Kheir, R.; Abdallah, C.; Khawlie, M. Assessing Soil Erosion in Mediterranean Karst Landscapes of Lebanon Using Remote Sensing and GIS. *Eng. Geol.* **2008**, *99*, 239–254. [CrossRef]
8. Nekhay, O.; Arriaza, M.; Boerboom, L. Evaluation of Soil Erosion Risk Using Analytic Network Process and GIS: A Case Study from Spanish Mountain Olive Plantations. *J. Environ. Manag.* **2009**, *90*, 3091–3104. [CrossRef] [PubMed]
9. Tongde, C.; Abbas, F.; Juying, J.; Ijaz, S.S.; Shoshan, A.; Ansar, M.; Hussain, Q.; Azad, M.N.; Ahmad, A. Investigation of Soil Erosion in Pothohar Plateau of Pakistan. *Pak. J. Agric. Res.* **2021**, *34*, 254–493. [CrossRef]
10. Ahmad, Z.; Butt, M.J. Environmental Study of Water Reservoirs for the Watershed Management in Pakistan. *Earth Syst. Environ.* **2019**, *3*, 613–623. [CrossRef]
11. Rather, M.A.; Satish Kumar, J.; Farooq, M.; Rashid, H. Assessing the Influence of Watershed Characteristics on Soil Erosion Susceptibility of Jhelum Basin in Kashmir Himalayas. *Arab. J. Geosci.* **2017**, *10*, 59. [CrossRef]
12. Dissanayake, D.; Morimoto, T.; Ranagalage, M. Accessing the Soil Erosion Rate Based on RUSLE Model for Sustainable Land Use Management: A Case Study of the Kotmale Watershed, Sri Lanka. *Model Earth Syst. Environ.* **2019**, *5*, 291–306. [CrossRef]
13. Haider, H.; Zaman, M.; Liu, S.; Saifullah, M.; Usman, M.; Chauhdary, J.N.; Anjum, M.N.; Waseem, M. Appraisal of Climate Change and Its Impact on Water Resources of Pakistan: A Case Study of Mangla Watershed. *Atmosphere* **2020**, *11*, 1071. [CrossRef]
14. Aziz, T. Changes in Land Use and Ecosystem Services Values in Pakistan, 1950–2050. *Environ. Dev.* **2021**, *37*, 100576. [CrossRef]
15. Shihong, L.; Wusheng, X.; Xiankun, L.; Runqin, T. A Review of Vegetation Restoration in Eroded Area of Red Soil. *Guangxi Zhiwu* **2003**, *23*, 83–89.
16. Jiao, J.; Zou, H.; Jia, Y.; Wang, N. Research Progress on the Effects of Soil Erosion on Vegetation. *Acta Ecol. Sin.* **2009**, *29*, 85–91. [CrossRef]
17. Guerrero-Campo, J.; Montserrat-Martí, G. Effects of Soil Erosion on the Floristic Composition of Plant Communities on Marl in Northeast Spain. *J. Veg. Sci.* **2000**, *11*, 329–336. [CrossRef]
18. Hewett, C.J.M.; Simpson, C.; Wainwright, J.; Hudson, S. Communicating Risks to Infrastructure Due to Soil Erosion: A Bottom-up Approach. *Land Degrad. Dev.* **2018**, *29*, 1282–1294. [CrossRef]

19. Borrelli, P.; Robinson, D.A.; Panagos, P.; Lugato, E.; Yang, J.E.; Alewell, C.; Wuepper, D.; Montanarella, L.; Ballabio, C. Land Use and Climate Change Impacts on Global Soil Erosion by Water (2015–2070). *Proc. Natl. Acad. Sci. USA* **2020**, *117*, 21994–22001. [CrossRef]
20. Dubois, O. *The State of the World's Land and Water Resources for Food and Agriculture: Managing Systems at Risk*; Earthscan: Oxford, UK, 2011.
21. Wuepper, D.; Borrelli, P.; Finger, R. Countries and the Global Rate of Soil Erosion. *Nat. Sustain.* **2020**, *3*, 51–55. [CrossRef]
22. Yang, D.; Kanae, S.; Oki, T.; Koike, T.; Musiake, K. Global Potential Soil Erosion with Reference to Land Use and Climate Changes. *Hydrol. Process.* **2003**, *17*, 2913–2928. [CrossRef]
23. Alewell, C.; Ringeval, B.; Ballabio, C.; Robinson, D.A.; Panagos, P.; Borrelli, P. Global Phosphorus Shortage Will Be Aggravated by Soil Erosion. *Nat. Commun.* **2020**, *11*, 4546. [CrossRef]
24. Ullah, S.; Syed, N.M.; Gang, T.; Noor, R.S.; Ahmad, S.; Waqas, M.M.; Shah, A.N.; Ullah, S. Recent Global Warming as a Proximate Cause of Deforestation and Forest Degradation in Northern Pakistan. *PLoS ONE* **2022**, *17*, e0260607. [CrossRef]
25. FAO. *Proceedings of the Global Symposium on Soil Erosion*; FAO: Rome, Italy, 2019.
26. Ganasri, B.P.; Ramesh, H. Assessment of Soil Erosion by RUSLE Model Using Remote Sensing and GIS—A Case Study of Nethravathi Basin. *Geosci. Front.* **2016**, *7*, 953–961. [CrossRef]
27. Fistikoglu, O.; Harmancioglu, N.B. Integration of GIS with USLE in Assessment of Soil Erosion. *Water Resour. Manag.* **2002**, *16*, 447–467. [CrossRef]
28. De Jong, S.M.; Paracchini, M.L.; Bertolo, F.; Folving, S.; Megier, J.; de Roo, A.P.J. Regional Assessment of Soil Erosion Using the Distributed Model SEMMED and Remotely Sensed Data. *Catena* **1999**, *37*, 291–308. [CrossRef]
29. Prasad, B.; Tiwari, H.L. A Comparative Study of Soil Erosion Models Based on GIS and Remote Sensing. *ISH J. Hydraul. Eng.* **2022**, *28*, 98–102. [CrossRef]
30. Batista, P.V.G.; Davies, J.; Silva, M.L.N.; Quinton, J.N. On the Evaluation of Soil Erosion Models: Are We Doing Enough? *Earth Sci. Rev.* **2019**, *197*, 102898. [CrossRef]
31. Boardman, J. Soil Erosion Science: Reflections on the Limitations of Current Approaches. *Catena* **2006**, *68*, 73–86. [CrossRef]
32. Choudhury, B.U.; Nengzouzam, G.; Islam, A. Runoff and Soil Erosion in the Integrated Farming Systems Based on Micro-Watersheds under Projected Climate Change Scenarios and Adaptation Strategies in the Eastern Himalayan Mountain Ecosystem (India). *J. Environ. Manag.* **2022**, *309*, 114667. [CrossRef]
33. Lew, R.; Dobre, M.; Srivastava, A.; Brooks, E.S.; Elliot, W.J.; Robichaud, P.R.; Flanagan, D.C. WEPPcloud: An Online Watershed-Scale Hydrologic Modeling Tool. Part I. Model Description. *J. Hydrol.* **2022**, *608*, 127603. [CrossRef]
34. Afonso de Oliveira Serrão, E.; Silva, M.T.; Ferreira, T.R.; Paiva de Ataide, L.C.; Assis dos Santos, C.; Meiguins de Lima, A.M.; de Paulo Rodrigues da Silva, V.; de Assis Salviano de Sousa, F.; Cardoso Gomes, D.J. Impacts of Land Use and Land Cover Changes on Hydrological Processes and Sediment Yield Determined Using the SWAT Model. *Int. J. Sediment Res.* **2022**, *37*, 54–69. [CrossRef]
35. Morgan, R.P.C. A Simple Approach to Soil Loss Prediction: A Revised Morgan-Morgan-Finney Model. *Catena* **2001**, *44*, 305–322. [CrossRef]
36. Koirala, P.; Thakuri, S.; Joshi, S.; Chauhan, R. Estimation of Soil Erosion in Nepal Using a RUSLE Modeling and Geospatial Tool. *Geosciences* **2019**, *9*, 147. [CrossRef]
37. Panagos, P.; Ballabio, C.; Himics, M.; Scarpa, S.; Matthews, F.; Bogonos, M.; Poesen, J.; Borrelli, P. Projections of Soil Loss by Water Erosion in Europe by 2050. *Environ. Sci. Policy* **2021**, *124*, 380–392. [CrossRef]
38. Kebede, Y.S.; Endalamaw, N.T.; Sinshaw, B.G.; Atinkut, H.B. Modeling Soil Erosion Using RUSLE and GIS at Watershed Level in the Upper Beles, Ethiopia. *Environ. Chall.* **2021**, *2*, 100009. [CrossRef]
39. Wischmeier, W.H.; Smith, D.D. *Predicting Rainfall Erosion Losses—A Guide to Conservation Planning. No. 537*; Department of Agriculture, Science and Education Administration: Washington, DC, USA, 1978.
40. Renard, K.; Foster, G.; Weesies, G.; McCool, D.; Yoder, D. *Predicting Soil Erosion by Water: A Guide to Conservation Planning with the Revised Universal Soil Loss Equation (RUSLE)*; United States Government Printing: Washington, DC, USA, 1997.
41. Jha, M.K.; Paudel, R.C. Erosion Predictions by Empirical Models in a Mountainous Watershed in Nepal. *J. Spat. Hydrol.* **2010**, *6*, 89–102.
42. Meliho, M.; Khattabi, A.; Mhammdi, N. Spatial Assessment of Soil Erosion Risk by Integrating Remote Sensing and GIS Techniques: A Case of Tensift Watershed in Morocco. *Environ. Earth Sci.* **2020**, *79*, 207. [CrossRef]
43. Boardman, J.; Shepheard, M.L.; Walker, E.; Foster, I.D.L. Soil Erosion and Risk-Assessment for on- and off-Farm Impacts: A Test Case Using the Midhurst Area, West Sussex, UK. *J. Environ. Manag.* **2009**, *90*, 2578–2588. [CrossRef]
44. Sandeep, P.; Kumar, K.C.A.; Haritha, S. Risk Modelling of Soil Erosion in Semi-Arid Watershed of Tamil Nadu, India Using RUSLE Integrated with GIS and Remote Sensing. *Environ. Earth Sci.* **2021**, *80*, 511. [CrossRef]
45. Dutta, D.; Das, S.; Kundu, A.; Taj, A. Soil Erosion Risk Assessment in Sanjal Watershed, Jharkhand (India) Using Geo-Informatics, RUSLE Model and TRMM Data. *Model Earth Syst. Environ.* **2015**, *1*, 37. [CrossRef]
46. Whittington, D. Improving the Performance of Contingent Valuation Studies in Developing Countries. *Environ. Resour. Econ.* **2002**, *22*, 323–367. [CrossRef]
47. Morgan, R.P.C.; Morgan, D.D.V.; Finney, H.J. A Predictive Model for the Assessment of Soil Erosion Risk. *J. Agric. Eng. Res.* **1984**, *30*, 245–253. [CrossRef]

48. Dou, X.; Ma, X.; Zhao, C.; Li, J.; Yan, Y.; Zhu, J. Risk Assessment of Soil Erosion in Central Asia under Global Warming. *Catena* **2022**, *212*, 106056. [CrossRef]
49. Ahmad, N.; Chaudhry, G.R. *Irrigated Agriculture of Pakistan*; Nazir, S., Ed.; Shahzad Nazir: Lahore, Pakistan, 1988.
50. Archer, D.R.; Fowler, H.J. Using Meteorological Data to Forecast Seasonal Runoff on the River Jhelum, Pakistan. *J. Hydrol.* **2008**, *361*, 10–23. [CrossRef]
51. Meraj, G.; Romshoo, S.A.; Yousuf, A.R.; Altaf, S.; Altaf, F. Assessing the Influence of Watershed Characteristics on the Flood Vulnerability of Jhelum Basin in Kashmir Himalaya. *Nat. Hazards* **2015**, *77*, 153–175. [CrossRef]
52. Doulabian, S.; Shadmehri Toosi, A.; Humberto Calbimonte, G.; Ghasemi Tousi, E.; Alaghmand, S. Projected Climate Change Impacts on Soil Erosion over Iran. *J. Hydrol.* **2021**, *598*, 126432. [CrossRef]
53. Alitane, A.; Essahlaoui, A.; el Hafyani, M.; el Hmaidi, A.; el Ouali, A.; Kassou, A.; el Yousfi, Y.; van Griensven, A.; Chawanda, C.J.; van Rompaey, A. Water Erosion Monitoring and Prediction in Response to the Effects of Climate Change Using RUSLE and SWAT Equations: Case of R'Dom Watershed in Morocco. *Land* **2022**, *11*, 93. [CrossRef]
54. Wang, J.; Lu, P.; Valente, D.; Petrosillo, I.; Babu, S.; Xu, S.; Li, C.; Huang, D.; Liu, M. Analysis of Soil Erosion Characteristics in Small Watershed of the Loess Tableland Plateau of China. *Ecol. Indic.* **2022**, *137*, 108765. [CrossRef]
55. Bensekhria, A.; Bouhata, R. Assessment and Mapping Soil Water Erosion Using RUSLE Approach and GIS Tools: Case of Oued El-Hai Watershed, Aurès West, Northeastern of Algeria. *ISPRS Int. J. Geoinf.* **2022**, *11*, 84. [CrossRef]
56. USGS. USGS EROS Archive—Digital Elevation—Shuttle Radar Topography Mission (SRTM) 1 Arc-Second Global. Available online: https://earthexplorer.usgs.gov/ (accessed on 11 November 2022).
57. FAO/Unesco. *Soil Map of the World 1:5,000,000 South Asia*; Food and Agriculture Organization: Rome, Italy, 1977; Volume 7, ISBN 92-3-101344-0.
58. Harris, I.; Osborn, T.J.; Jones, P.; Lister, D. Version 4 of the CRU TS Monthly High-Resolution Gridded Multivariate Climate Dataset. *Sci. Data* **2020**, *7*, 109. [CrossRef]
59. Azimi Sardari, M.R.; Bazrafshan, O.; Panagopoulos, T.; Sardooi, E.R. Modeling the Impact of Climate Change and Land Use Change Scenarios on Soil Erosion at the Minab Dam Watershed. *Sustainability* **2019**, *11*, 3353. [CrossRef]
60. Pradhan, B.; Chaudhari, A.; Adinarayana, J.; Buchroithner, M.F. Soil Erosion Assessment and Its Correlation with Landslide Events Using Remote Sensing Data and GIS: A Case Study at Penang Island, Malaysia. *Environ. Monit. Assess* **2012**, *184*, 715–727. [CrossRef]
61. Nearing, M.A.; Pruski, F.F.; O'Neal, M.R. Expected Climate Change Impacts on Soil Erosion Rates: A Review. *J. Soil Water Conserv.* **2004**, *59*, 43–50.
62. Li, B.; Shi, X.; Lian, L.; Chen, Y.; Chen, Z.; Sun, X. Quantifying the Effects of Climate Variability, Direct and Indirect Land Use Change, and Human Activities on Runoff. *J. Hydrol.* **2020**, *584*, 124684. [CrossRef]
63. Sharpley, A.N. Depth of Surface Soil-runoff Interaction as Affected by Rainfall, Soil Slope, and Management. *Soil Sci. Soc. Am. J.* **1985**, *49*, 1010–1015. [CrossRef]
64. Arnoldus, H.M.J.; de Boodt, M.; Gabriels, D. *An Approximation of the Rainfall Factor in the Universal Soil Loss Equation*; John Wiley and Sons Ltd.: Chichester, UK, 1980.
65. Williams, J.R. Chapter 25. The EPIC Model. In *Computer Models of Watershed Hydrology*; Singh, V.P., Ed.; Water Resources Publications: Littleton, CO, USA, 1995.
66. Siswanto, S.Y.; Sule, M.I.S. The Impact of Slope Steepness and Land Use Type on Soil Properties in Cirandu Sub-Sub Catchment, Citarum Watershed. In Proceedings of the IOP Conference Series: Earth and Environmental Science; IOP Publishing: Bristol, UK, 2019; Volume 393.
67. McCool, D.K.; Brown, L.C.; Foster, G.R.; Mutchler, C.K.; Meyer, L.D. Revised Slope Steepness Factor for the Universal Soil Loss Equation. *Trans. ASAE* **1987**, *30*, 1387–1396. [CrossRef]
68. Moore, I.D.; Burch, G.J. Modelling Erosion and Deposition: Topographic Effects. *Trans. ASAE* **1986**, *29*, 1624–1630. [CrossRef]
69. Moore, I.D.; Burch, G.J. Physical Basis of the Length-Slope Factor in the Universal Soil Loss Equation. *Soil Sci. Soc. Am. J.* **1986**, *50*, 1294–1298. [CrossRef]
70. Vatandaşlar, C.; Yavuz, M. Modeling Cover Management Factor of RUSLE Using Very High-Resolution Satellite Imagery in a Semiarid Watershed. *Environ. Earth Sci.* **2017**, *76*, 65. [CrossRef]
71. Durigon, V.L.; Carvalho, D.F.; Antunes, M.A.H.; Oliveira, P.T.S.; Fernandes, M.M. NDVI Time Series for Monitoring RUSLE Cover Management Factor in a Tropical Watershed. *Int. J. Remote. Sens.* **2014**, *35*, 441–453. [CrossRef]
72. Wischmeier, W.H.; Johnson, C.B.; Cross, B.V. Soil Erodibility Nomograph for Farmland and Construction Sites. *J. Soil Water Conserv.* **1971**, *26*, 189–193.
73. Ekwueme, O.U.; Obiora, D.N.; Okeke, F.N.; Ibuot, J.C. Environmental Assessment of Gully Erosion in Parts of Enugu North, Southeastern Nigeria. *Indian J. Sci. Technol.* **2021**, *14*, 2400–2409. [CrossRef]
74. Kalambukattu, J.; Kumar, S. Modelling Soil Erosion Risk in a Mountainous Watershed of Mid-Himalaya by Integrating RUSLE Model with GIS. *Eurasian J. Soil Sci. (EJSS)* **2017**, *6*, 92. [CrossRef]
75. Borrelli, P.; Robinson, D.A.; Fleischer, L.R.; Lugato, E.; Ballabio, C.; Alewell, C.; Meusburger, K.; Modugno, S.; Schütt, B.; Ferro, V.; et al. An Assessment of the Global Impact of 21st Century Land Use Change on Soil Erosion. *Nat. Commun.* **2017**, *8*, 2013. [CrossRef] [PubMed]

76. Gilani, H.; Ahmad, A.; Younes, I.; Abbas, S. Impact Assessment of Land Cover and Land Use Changes on Soil Erosion Changes (2005–2015) in Pakistan. *Land Degrad. Dev.* **2022**, *33*, 204–217. [CrossRef]
77. Aslam, M.H.; Yoshimura, K. Sediment Yield in Jhelum River Basin with and without Climate Change Impact in Pakistan. *J. Jpn. Soc. Civ. Eng. Ser. B1* **2017**, *73*, 85–90. [CrossRef]
78. Ashraf, A.; Abuzar, M.K.; Ahmad, B.; Ahmad, M.M.; Hussain, Q. Modeling Risk of Soil Erosion in High and Medium Rainfall Zones of Pothwar Region, Pakistan. *Proc. Pak. Acad. Sci. Part B* **2017**, *54*, 67–77.
79. Mahmood, R.; Jia, S. Assessment of Impacts of Climate Change on the Water Resources of the Transboundary Jhelum River Basin of Pakistan and India. *Water* **2016**, *8*, 246. [CrossRef]
80. Kamp, U.; Growley, B.J.; Khattak, G.A.; Owen, L.A. GIS-Based Landslide Susceptibility Mapping for the 2005 Kashmir Earthquake Region. *Geomorphology* **2008**, *101*, 631–642. [CrossRef]
81. Shafique, M.; van der Meijde, M.; Khan, M.A. A Review of the 2005 Kashmir Earthquake-Induced Landslides; from a Remote Sensing Prospective. *J. Asian Earth Sci.* **2016**, *118*, 68–80. [CrossRef]
82. Bureau of Statistics. Booklet, AJ&K at A Glance, Government of the State of Azad Jammu & Kashmir. 2021. Available online: https://pndajk.gov.pk/uploadfiles/downloads/AJ&KAtAGlance-2021.pdf (accessed on 20 February 2023).
83. Pimentel, D.; Burgess, M. Soil Erosion Threatens Food Production. *Agriculture* **2013**, *3*, 443–463. [CrossRef]
84. FAO. *Asia-Pacific Forests and Forestry to 2020*; FAO: Rome, Italy, 2010; ISBN 978-92-5-106566-2.
85. Bezak, N.; Mikoš, M.; Borrelli, P.; Alewell, C.; Alvarez, P.; Anache, J.A.A.; Baartman, J.; Ballabio, C.; Biddoccu, M.; Cerdà, A.; et al. Soil Erosion Modelling: A Bibliometric Analysis. *Environ. Res.* **2021**, *197*, 111087. [CrossRef]
86. Borrelli, P.; Alewell, C.; Alvarez, P.; Anache, J.A.A.; Baartman, J.; Ballabio, C.; Bezak, N.; Biddoccu, M.; Cerdà, A.; Chalise, D.; et al. Soil Erosion Modelling: A Global Review and Statistical Analysis. *Sci. Total Environ.* **2021**, *780*, 146494. [CrossRef] [PubMed]
87. Li, C.; Lu, T.; Wang, S.; Xu, J. Coupled Thorens and Soil Conservation Service Models for Soil Erosion Assessment in a Loess Plateau Watershed, China. *Remote. Sens.* **2023**, *15*, 803. [CrossRef]
88. Stone, R.P.; Hilborn, D. *Factsheet, Universal Soil Loss Equation (USLE)*; Ministry of Agriculture, Food and Rural Affairs: Guelph, ON, Canada, 2000. Available online: http://www.omafra.gov.on.ca/english/engineer/facts/12-051.htm (accessed on 22 November 2022).
89. Hurni, H. Soil Erosion in Huai Thung Choa-Northern Thailand Concerns and Constraints. *Mt. Res. Dev.* **1982**, *2*, i + 141–156. [CrossRef]
90. Carter, M.R. Conservation Tillage. *Encycl. Soils Environ.* **2004**, *4*, 306–311. [CrossRef]